Nov 24th, 12:00 AM

The Local Instability of Thin-walled Sections under Combined Compression and Bending

J. Rhodes

James M. Harvey

THE LOCAL INSTABILITY OF THIN-WALLED SECTIONS UNDER COMBINED COMPRESSION AND BENDING

by

J. Rhodes, B.Sc., PhD.*

and

J.M. Harvey, B.Sc.,MS.,Ph.D.,A.R.C.S.T.,C.Eng.,F.I.Mech.E.†

*Lecturer, Department of Mechanics of Materials, University of Strathclyde, Glasgow.

†Professor, Department of Mechanics of Materials, University of Strathclyde, Glasgow.

INTRODUCTION

The problem of local buckling of thin plates and thin walled structural sections under direct compression has interested investigators for the past four or five decades. Bleich (1), Lundquist and Stowell (7), Chilver (3), Harvey (4), Bulson (2), Wittrick (15), and many others, have presented solutions for a variety of problems in this field. The action of a combination of bending moments and direct compression on a section, however, has received relatively little attention.

Solutions to the problem of a single plate under compression and moments in its plane have been obtained by several researchers, including Timoshenko (12), Schuette and McCulloch (11), Johnson and Noel (5) and Walker (13) (14). Johnson and Noel advocated that their results should be used in conjunction with tables published by Kroll (6) in order to evaluate buckling loads for sections under eccentrically applied loading. Walker found buckling loads for plain and lipped channel sections under compression and bending about an axis parallel to the web by using a graphical method to link the behaviour of component plates. Harvey investigated the case of a channel under pure bending about the axis of symmetry using an approximate solution for the flanges. All the solutions taking moments into account are indirect and make use of procedures to link the component plates which have been investigated individually. (A recent paper by Plank and Wittrick (17) gives buckling stresses for plain channels in bending about the axis of symmetry obtained using a complex finite strip method of analysis.)

The greatest difficulty encountered in the solution of this type of problem is found in determining the restraint imposed by adjacent plates on each other. The analysis presented in this paper makes no

attempt to calculate the restraints on each plate, but allows each plate to deform in any number of ways compatible with the deformations of its adjacent plates. The rotational restraint theoretically imposed on adjacent plates at the junctions is changed for each prescribed set of deflection functions which cover the whole section so that the analysis allows a high degree of freedom at the junctions. The Principle of Minimum Potential Energy is then employed to establish the relative magnitude of the prescribed deflection functions to give the lowest possible buckling load for the section. Knowing the deflected form of the section the rotational restraints imposed between adjacent plates can be evaluated if required.

The buckling solution so obtained can then be used as a starting point for analysis of the post-buckling behaviour of the section. This procedure has been used by the authors in a number of post-buckling analyses (8)(9)(10). The post-buckling analysis is not detailed in this paper, although the problem is discussed and some results are shown.

BUCKLING ANALYSIS

Consider the section shown in Fig. 1. A plain channel section is shown for illustration but the same approach has been used for lipped channel and trapezoidal sections. A force P is applied through the centroid, and a moment M acts about the neutral axis of bending. It is assumed that the load acts on the ends of the section through rigid plates which prevent warping of the ends.

The stress system due to the applied loading will therefore be as

shown in the figure. On the web the stress is constant with magnitude denoted $\bar{\sigma}$. On the flanges the effect of the applied moment is to cause a variation in stress across the flange. The variation in stress across the section can be taken into account using the factor α indicated in Fig. 1. On the flanges the stress variation is $\bar{\sigma}(1-\alpha y_2/b_2)$. In the case of a lipped channel the factor α can also be used to obtain the lip stresses in terms of the web stress by writing $\sigma_{lip} = \bar{\sigma}(1-\alpha)$.

Thus the stresses in all plates can be found in terms of the web stress $\bar{\sigma}$, which is used as a reference stress.

The problem now requires the evaluation of the magnitude of $\bar{\sigma}$ to cause local buckling of the section. The evaluation of $\bar{\sigma}$ can be obtained from an examination of the potential energy of the system at the point of buckling as follows.

The work done, U , by the external loads and moments in the locally buckled strut can be expressed in terms of the local deflections and the edge stresses (see ref. 8).

$$U = -\sum_{i=1}\iint \frac{t}{2}.\bar{\sigma} \times \left(1 - \frac{\alpha_i . y_i}{b_i}\right)\left(\frac{\partial w_i}{\partial x}\right)^2 dy_i dx \qquad (1)$$

and the strain energy contained in the section due to bending is

$$V_1 = \sum_{i=1}\iint \frac{D}{2}\left\{\left[\frac{\partial^2 w_i}{\partial x^2} + \frac{\partial^2 w_i}{\partial y_i^2}\right]^2 - 2(1-\nu)\left[\frac{\partial^2 w_i}{\partial y_i^2}.\frac{\partial^2 w_i}{\partial x^2} - \left(\frac{\partial^2 w_i}{\partial x \partial y_i}\right)^2\right]\right\} dy_i \; dx \qquad (2)$$

The potential energy of the system is the sum of U and V_1.

i.e. $$V = U + V_1 \qquad (3)$$

To evaluate the potential energy, the form of the local deflections w_i, must be specified for all plates of the section. The plate

loaded ends are assumed to be simply supported and the very small curvatures of the plate edge due to the moments are neglected so that the buckles vary sinusoidally in the x-direction

$$\text{i.e.} \qquad w_i = \sin\frac{\pi x}{eb_1} \sum_{n=1}^{N} A_n Y_{in} \tag{4}$$

Note that the period of the buckles is the same for all plates, from conditions of compatibility, and is related to the width of the reference plate by the constant e.

The functions Y_{in} are dependent on y_i only and must satisfy the boundary conditions at the plate edges. These functions were postulated as algebraic polynomials. The construction of a set of functions is illustrated here for a plane channel strut with co-ordinate system as shown in Fig. 2, and similar functions are obtained for lipped channel sections using different boundary conditions.

On the web, a typical function Y_{1n} is

$$Y_{1n} = \left[\left(\frac{y_1}{b}\right)^{f_{1n}} + \beta_{1n}\left(\frac{y_1}{b}\right)^{g_{1n}} + \gamma_{1n}\left(\frac{y_1}{b}\right)^{\ell_{1n}} \right] \tag{5}$$

On the flanges, the corresponding function chosen is

$$Y_{2n} = C_n\left[\left(\frac{hy_2}{b}\right) + \beta_{2n}\left(\frac{hy_2}{b}\right)^2 + \gamma_{2n}\left(\frac{hy_2}{b}\right)^{f_{2n}} + \delta_{2n}\left(\frac{hy_2}{b}\right)^{g_{2n}}\right] \tag{6}$$

where $b = \frac{b_1}{2}$, $h = \frac{b}{b_2}$ and C_{2n} is a magnitude coefficient

The indices f_{1n}, g_{1n} and ℓ_{1n} are arbitrary integers and are even to ensure symmetry of web deflections. In at least one function Y_{1n} used in the series the lowest index, say f_{1n} is taken as zero to ensure that deflections are allowed to exist on the web centre line.

The indices f_{2n} and g_{2n} are also arbitrary in magnitude and may be even or odd integers.

The functions Y_{1n} and Y_{2n} must be related to satisfy the boundary conditions at the plate junctions and at the free edges of the flanges. These conditions are as follows.

At the web/flange junction small out of plane deflections which exist due to curvature of the section are neglected and the deflections are assumed to be zero. Also the slopes of the plates must be equal to ensure compatibility and the moments imposed by one plate on another must be resisted by an equal moment. These conditions can be expressed:-

$$w_1 = w_2 = 0$$

$$\frac{\partial w_1}{\partial y_1} = \frac{\partial w_2}{\partial y_2} \qquad (7)$$

$$-D\left[\frac{\partial^2 w_1}{\partial y_1^2} + \nu\frac{\partial^2 w_1}{\partial x^2}\right] = -D\left[\frac{\partial^2 w_2}{\partial y_2^2} + \nu\frac{\partial^2 w_2}{\partial x^2}\right]$$

at $y_1 = b$, $y_2 = 0$.

At the free edges of the flanges the conditions of zero moment and zero shear exist. These conditions may be expressed

$$-D\left[\frac{\partial^2 w_2}{\partial y_2^2} + \nu\frac{\partial^2 w_2}{\partial x^2}\right] = 0$$

$$-D\left[\frac{\partial^3 w_2}{\partial y_2^3} + (2-\nu)\frac{\partial^3 w_2}{\partial y_2 \partial x^2}\right] = 0 \qquad (8)$$

at $y_2 = b_2$.

Using equation 4 and introducing the term $\frac{R_n}{b_1}$, which may be defined as the coefficient of restraint for the nth term, allows the conditions (7) and (8) to be expressed in terms of the functions Y_{in} as follows

$$\begin{aligned} Y_{1n} &= Y_{2n} = 0 \\ Y'_{1n} &= Y'_{2n} \\ \frac{Y''_{1n}}{Y'_{1n}} &= \frac{Y''_{2n}}{Y'_{2n}} = \frac{R_n}{b_1} \end{aligned} \tag{9}$$

at $y_1 = b$, $y_2 = 0$

$$\begin{aligned} Y''_{2n} - \nu\frac{\pi^2}{e^2b^2} Y_{2n} &= 0 \\ Y'''_{2n} - (2-\nu)\frac{\pi^2}{e^2b^2} Y'_{2n} &= 0 \end{aligned} \tag{10}$$

at $y_2 = b_2$

The coefficient $\frac{R_n}{b_1}$ has no specified value and is arbitrarily prescribed, different values of this coefficient being used for each term 'n', so that a large degree of freedom is allowed at the junctions.

Equations (9) and (10) can be satisfied for any arbitrarily prescribed values of the indices if the coefficients have the following magnitudes

$$\gamma_{1n} = \frac{f_{1n}(f_{1n}-1) - g_{1n}(g_{1n}-1) + \frac{R_n}{b_1}(g_{1n}-f_{1n})}{g_{1n}(g_{1n}-1) - \ell_{1n}(\ell_{1n}-1) + \frac{R_n}{b_1}(\ell_{1n}-g_{1n})}$$

$$\beta_{1n} = -(1+\gamma_{1n})$$

$$c_n = \frac{1}{h}(f_{1n} + g_{1n}\cdot\beta_{1n} + \ell_{1n}\cdot\gamma_{1n})$$

$$\beta_{2n} = \frac{R_n}{2h} \qquad (11a,b,c,d,e,f)$$

$$\delta_{2n} = \frac{1^* + \beta_{2n}\cdot 2^*\cdot\dfrac{f_{2n}^{**}}{f_{2n}} - (1^{**} + \beta_{2n} \times 2^{**})}{f_{2n}^{**} - g_{2n}{}^*\dfrac{f_{2n}^{**}}{f_{2n}^*}}$$

and

$$\gamma_{2n} = -1^* + \beta_{2n}\cdot 2^* + \delta_{2n}\cdot g_{2n}{}^* / f_{2n}{}^*$$

where $k^* = \frac{1}{b^3}k(k-1)(k-2) - (2-\nu)\frac{\pi^2}{e^2b^2}\frac{k}{b}$

and $k^{**} = \frac{k}{b^2}(k-1) - \nu\frac{\pi^2}{e^2b^2}$ for any coefficient k.

Thus a suitable deflection form for all plates is specified with conditions at all boundaries satisfied. This constitutes the nth term of the deflection series, each item of the series prescribing deflected forms for all plates. By altering the indices f_{1n} etc. and the coefficient $\frac{R_n}{b_1}$ and substituting in equations (11) alternative sets of suitable deflection functions can be obtained to make up any required number of terms in the deflection series.

Each term in the series is assigned a magnitude coefficient and the series, $\Sigma A_n Y_{in}$ is therefore formed. Similar, if somewhat

more lengthy, sets of functions can be generated for the other sections discussed using the same approach.

Having obtained forms for the local deflections across the section, the analysis can be completed using the Principle of Minimum Potential Energy.

The potential energy of the system can be expressed in terms of the coefficients A_n. Substituting for w_i from equation (4) into equations (1) and (2), adding and integrating in the x-direction gives for the potential energy of the system

$$V = \sum_{n=1}^{N} \sum_{m=1}^{N} A_n . A_m \left[\frac{aD\pi^2}{4b_1^2} . Q_{nm} - \bar{\sigma} . \frac{at}{4} . S_{nm} \right] \tag{12}$$

where

$$Q_{nm} = \sum_{i=1,2,3} \left\{ \int_0^{b_i} (Y''_{in} - \frac{\pi^2}{e^2 b_1^2} . Y_{in})(Y''_{im} - \frac{\pi^2}{e^2 b_1^2} . Y_{im}) \frac{b_1^2}{\pi^2} \, dy_i \right.$$

$$\left. -2(1-\nu) . \frac{1}{e^2} \left[Y_{in} . Y'_{im} \right]_0^{b_i} \right\} \tag{13}$$

$$S_{nm} = \sum_{i=1,2,3} \int_0^{b_i} (1 - \frac{\alpha_i . y_i}{b_i}) Y_{in} . Y_{im} . dy_i \tag{14}$$

In equation (14) $\alpha_1 = 0$, $\alpha_2 = \alpha_3 = \alpha$.

To find the value of $\bar{\sigma}$ corresponding to buckling the Principle of

Minimum Potential Energy is now used

i.e. $$\frac{\partial V}{\partial A_n} = 0$$

Applying this to equation (12) gives a series of N simultaneous equations for A_n of the form

$$\sum_{m=1}^{N} A_n \left(\frac{aD}{4} \cdot \frac{\pi^2}{b_1^2} Q_{nm} - \bar{\sigma} \frac{at}{4} . S_{nm}\right) = 0 \qquad (15)$$

It is obvious that equations (15) can also be written

$$\sum_{m=1}^{N} A_n (Q_{nm} - K_1 . S_{nm}) = 0$$

where K_1 is the non-dimensional form of $\bar{\sigma}$,

i.e. $$K_1 = \frac{\bar{\sigma} . b_1^2 . t}{\pi^2 D}$$

This series of simultaneous equations can be expressed in the following matrix form

$$\begin{bmatrix} (Q_{11}-K_1.S_{11}) & (Q_{12}-K_1.S_{12}) \cdots (Q_{1N}-K_1.S_{1N}) \\ (Q_{21}-K_1.S_{21}) & \cdots\cdots \\ & \\ & \\ & \\ (Q_{N1}-K_1.S_{N1}) & \cdots\cdots\cdots\cdots\cdots\cdots (Q_{NN}-K_1.S_{NN}) \end{bmatrix} \begin{bmatrix} A_1 \\ A_2 \\ \\ \\ \\ A_N \end{bmatrix} = 0$$

The non-trivial solutions of this set of equations furnish the values

of $\bar{\sigma}$ for the various modes of local buckling which can occur. In general the lowest eigenvalue of $\bar{\sigma}$ is that at which buckling occurs.

The required eigenvalue can be calculated by any of a number of numerical methods and the deflected forms of the various plates can be obtained if required from the corresponding eigenvector.

The buckling loads and moments can now be found from the value of $\bar{\sigma}$ obtained and thus the instability problem is solved. At this stage it should be pointed out that the solution obtained is dependent on the buckle half wavelength initially postulated, i.e. by the value of e prescribed. If the length 'a' of the section is such that there is more than one buckle then the half wavelength to give the lowest buckling stresses must be evaluated by obtaining solutions considering a number of buckle half wavelengths.

For the general case, for sections of unspecified length, the buckle half wavelength used should be that which gives the lowest possible buckling stresses. This can be evaluated very simply by inspection of the eigenvalues obtained for a number of values of buckle half wavelengths.

RESULTS

The variation in minimum local buckling stresses for plain channels under various loading eccentricities is shown in Fig. 3. The buckle half wavelength used was that which produced minimum K_1. It is emphasised here that these curves only apply to the case of local buckling and do not take into account the effects of other types of buckling, such as Euler buckling, or torsional buckling. For long struts, or struts with narrow flanges, Euler buckling may be

encountered prior to local buckling, and for channels with wide flanges there is a possibility of torsional buckling. These alternative buckling modes therefore must also be considered and various methods of analysis exist.

An indication of the effects of Euler buckling for uniformly compressed struts can be very easily obtained using the standard expression for Euler instability

$$\sigma_{CR} = \frac{P_{CR}}{A} = \frac{\pi^2 E}{(\frac{L}{r})^2} \qquad (16)$$

Figure 4 shows the effects of length on the initial buckling load for a uniformly compressed plain channel of a web width to thickness ratio equal to fifty. The local buckling curve is taken from Fig. 3 and the lines representing Euler buckling obtained from equation (16), rearranged to give results in terms of K_1.

Also shown are the results of Wittrick and Williams (16). The results of reference (16) were obtained from an extremely accurate analysis which obtains the minimum critical load considering all types of buckling. From the figure it can be seen that the use of equation (16) gives results in reasonable agreement with the rigorous analysis of reference (16) in the Euler buckling range. The value of Poisson's ratio used by the authors was 0.3 as compared with 0.36 used in reference (16), which accounts for some of the differences between the curves.

Figure 5 shows local buckling stresses for a lipped channel strut for various loading eccentricities. Again these are only for local

buckling and do not take into account other modes of buckling. In particular, in this case the effects which can occur if the lips are narrow and buckle laterally are neglected. The curves of Fig. 5 were drawn on the basis that the lips fulfil the function of making the deflections of the flanges zero at the flange-lip junction, and do not have any other effects on the local buckling behaviour. If the lips are very large, then the lips themselves will initiate buckling and the curves of Fig. 5 will over estimate the buckling stresses. Since the main purpose of this paper is to show the general effects of eccentric loading on local buckling, Fig. 5 illustrates these effects unobscured by the added complications ensuing from lip buckling.

An important case of eccentric loading arises when the eccentricity tends to infinity, i.e. when the section is loaded under pure bending. Figure 6 shows buckling coefficients for a lipped channel under pure bending. The applied moment is such that the web is in compression and the lips are in tension. The effects of lip bending are taken into account in this case and it can be observed from the figure that these effects are negligible. The corresponding values of the critical applied moment are shown in Fig. 7. Here it is seen that the effects of lip width on the critical moment are quite substantial because the I value of the section is dependent on lip width. It is interesting to note in passing that the critical moment for a section with a given material thickness is independent on the absolute magnitudes of the other dimensions, but depends only on the relative dimensions.

COMPARISON WITH EXPERIMENTAL RESULTS

The accuracy of the theoretical predictions can be assessed by

comparing the buckling loads with those obtained experimentally. A number of experiments were carried out to compare with theory, and some results are illustrated here.

A large scale investigation into the behaviour of beams under pure bending is reported in reference (9). Pure bending was applied to lipped channel and trapezoidal section beams over a six foot span and the buckling loads were obtained using strain gauges on the centre of the compression element (b_1). From the strain gauge readings a plot of membrane strain versus applied moment could be drawn for the centre of the compression element as shown in Fig. 8. Buckling was assumed to occur when tangents to the post-buckling and pre-buckling slopes of the membrane stress curve coincided as indicated in the figure.

Figure 9 shows a comparison of the experimental results thus obtained for trapezoidal sections with the theoretical predictions, and indicates that agreement is very satisfactory. It was observed during the tests that the point of buckling was very clearly defined for the beams tested, all membrane strain graphs giving sharp changes in slope at buckling, as shown in Fig. 8.

To obtain experimental results for plain and lipped channels under eccentric compression, a number of tests were carried out on short struts.

The struts tested were two feet long and all had webs of 8 inches width. The lip width of the lipped channels was kept constant at 1½ inches, and the material thickness used was nominally 0.048 inches. These dimensions were chosen so that buckling occurred purely in the local mode. The length of the struts was rather too short to let

the minimum buckle wavelength develop naturally, but was long enough to enable a choice of several wavelengths to be obtained.

Loads were applied through loading plates which produced approximately simply supported conditions at the plate ends, as shown diagramatically in Fig. 10. Any specified eccentricity of loading could be obtained by situating the adjustable knife edges through which loads were applied, at the required position relative to the web. Buckling loads were obtained, as for the beams, using strain gauges to obtain the variation of membrane strains. For plain channels two pairs of gauges were used, one pair at the flange free edges and the other pair on the web centre line. For the lipped channels only one pair of gauges were used and these were situated on the web centre line.

Figure 11 shows a comparison of theoretical and experimental buckling loads for lipped channels with loads applied at various eccentricities. The agreement is good, although the experimental loads are constantly a little lower than those predicted theoretically, despite the fact that the theoretical wavelength for minimum buckling load was unobtainable experimentally. It was observed in this case that the experimental buckling load was not so clearly defined as the beam experiments. This is mainly due to the combination of bending and direct stresses which tended to make initial imperfections grow quite rapidly and mask the buckling load to some extent, although the method used to obtain the buckling load was still able to cope adequately with these effects.

Figure 12 shows theoretical and experimental results for plain channel struts. In this case, only two loading conditions are shown, uniform compression and eccentricity of loading such that $\alpha = 1$. The results are again shown to be in very good agreement, thus verifying the accuracy of the theoretical solution.

EXTENSION OF ANALYSIS INTO THE POST-BUCKLING RANGE

It is well known that local buckling does not necessarily impose an upper limit to the carrying capacity of a thin-walled section, and many members can function satisfactorily well beyond the local buckling load. The analysis of local buckling can serve as a very useful initial step in the examination of section behaviour in the post-buckling range. From the buckling analysis a very accurate estimate of the deflected form of the section at buckling is obtained and this can be used in a subsequent large deflection analysis.

The authors have performed post-buckling analyses using the buckling solution as a first step for the case of beams and struts (9)(10). The results for beams have been compared with large numbers of experimental results, and show excellent agreement. The strut analysis has not been compared with experimental results for post-buckling behaviour, although as has been shown the buckling behaviour is accurately predicted by theory. An indication of the post-buckling behaviour predicted theoretically may be obtained from Fig. 13 which shows load-end displacement paths for lipped channels with various flange/web ratios loaded in uniform compression. The buckle half wavelengths used were those which gave minimum buckling load. As can be seen, the slope of the post-buckling curves is greatest if the flange widths are approximately half the web width. This is illustrated more clearly in Fig. 14 which shows the ratio of post-buckling to prebuckling stiffness of the struts against end compression. Also shown in this figure are the corresponding results for plain channels. The curve for plain channels is quite different from that for lipped channels. In the case of plain channels the post-buckling stiffness has a minimum when the flange/web ratio is about 0.35.

Around this flange/web ratio the flanges and the web buckle simultaneously with more or less simple support conditions at the boundaries. In the case of the lipped channels the ratio of post-buckling to prebuckling stiffness is at its lowest when the web and flange widths are approximately equal, which also indicates simultaneous flange and web buckling. Therefore in general it can be deduced that the reduction in section stiffness is a maximum if the component plates are of such dimensions that local buckling occurs simultaneously in all plates.

CONCLUSIONS

The buckling analysis has been shown to predict accurately the local buckling loads for plain channels, lipped channels and trapezoidal sections under combinations of bending and compression. No account is taken in the analysis of buckling in any mode other than the local buckling mode, so that the curves shown do not include the effects of Euler buckling, torsional buckling, etc.

The buckling analysis can be used as a first step in an examination of the post-buckling behaviour of a section. Further experimental work is required to evaluate the accuracy of the theoretical post-buckling predictions for struts, although the analysis has been shown in previous publications to be accurate for beam behaviour.

APPENDIX 1

References

1	Bleich, H H	"Buckling strength of metal structures" McGraw-Hill Book Co, Inc, 1952
2	Bulson, P S	"The stability of flat plates" Chatto & Windus, 1970
3	Chilver, A H	"The behaviour of thin-walled structural members in compression" Engineering, 1951
4	Harvey, J M	"Structural strength of thin-walled channel sections" Engineering, Vol CLXXV, 1953
5	Johnson, J H & Noel, R G	"Critical bending stresses for flat rectangular plates supported along all edges and elastically restrained against rotation along the unloaded compression edge" Jnl of the Aero Sciences, Vol 20, 1953
6	Kroll, W O	"Tables of stiffness and carry-over factors for flat rectangular plates under compression" NACA Arr No 3K27, 1943
7	Lundquist, E E & Stowell, E Z	"Critical compressive stresses for outstanding flanges" NACA Report No 809, 1945
8	Rhodes, J	"The non-linear behaviour of thin-walled beams" PhD thesis, University of Strathclyde, Glasgow, 1969
9	Rhodes, J & Harvey, J M	"The local buckling and post-local buckling behaviour of thin-walled beams" Aero Quarterly, Vol XXII, 1971
10	Rhodes, J & Harvey, J M	"Plain channel section struts in compression and bending beyond the local buckling load" Paper submitted for publication to the International Jnl of Mechanical Sciences
11	Schuette, E H & McCulloch, J C	"Charts for the minimum weight design of multiweb wings in bending" NACA TN No 1323, 1947
12	Timoshenko, S P & Gere, J M	"Theory of elastic stability" 2nd Ed, McGraw-Hill, 1961
13	Walker, A C	"Thin-walled structural forms under eccentric compressive load actions" PhD thesis, University of Glasgow, 1964
14	Walker, A C	"Local instability in plates and channel struts" Proc ASCE, Jnl of the structural Div, Vol 92, No ST3, 1966

15 Wittrick, W H "A unified approach to the initial buckling of stiffened panels in compression" Aeronautical Quarterly, Vol XIX, 1968

16 Wittrick, W H & Williams, F W "Initial buckling of channels in compression" Proc ASCE Jnl of the Engineering Mechanics Div, Vol 97, No EM3, 1971

17 Plank, R J & Wittrick, W H "Buckling under combined loading of thin, flat-walled structures by a complex finite strip method" International Jnl for Numerical Methods in Engineering, Vol 8, 1974

APPENDIX 2

Notation	Coefficient
A_n	Coefficient
b_i	Width of the ith plate
D	Plate flexural rigidity factor ($= \frac{Et^3}{12(1-\nu^2)}$)
E	Young's modulus of rigidity
e	Ratio of buckle half-wavelength to half width of reference plate
I_y, I_z	Second moments of area about the y and z axes
M	Moment
P	Load
t	Thickness of plate
x, y_i, z	Co-ordinates
Y_i	Deflected form across the ith plate
w_i	Deflections in the ith plate
α	Factor prescribing eccentricity of stress variation
σ_x	Stress in the x-direction
$\bar{\sigma}$	Stress in the x-direction in the reference plate

ν	Poisson's ratio (taken as 0.3 for all numerical calculations)
$f_{1n}, g_{1n}, \ell_{1n} f_{2n}, g_{2n}$	Indices used in deflection functions
$\beta_{1n}, \gamma_{1n}, \beta_{2n}, \delta_{2n}, c_n$	Coefficients used in deflection functions

Other symbols are defined where they first appear in the text.

Primes denote differentiation with respect to y_i

$$\text{e.g. } Y''_{in} = \frac{d^2 Y_{in}}{dy_i^2}$$

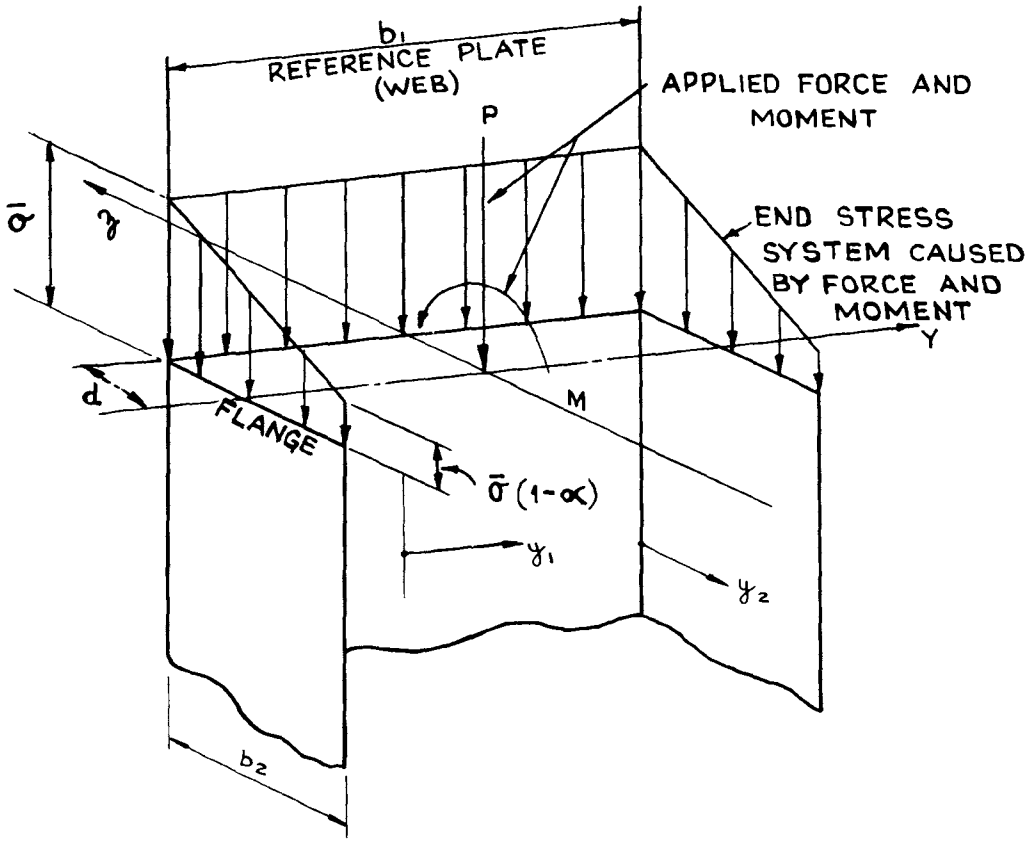
b1
REFERENCE PLATE
(WEB)
P
APPLIED FORCE AND
MOMENT
σ̄
y
END STRESS
SYSTEM CAUSED
BY FORCE AND
MOMENT
Y
d
FLANGE
M
σ̄ (1-α)
y1
y2
b2

FIG. 1

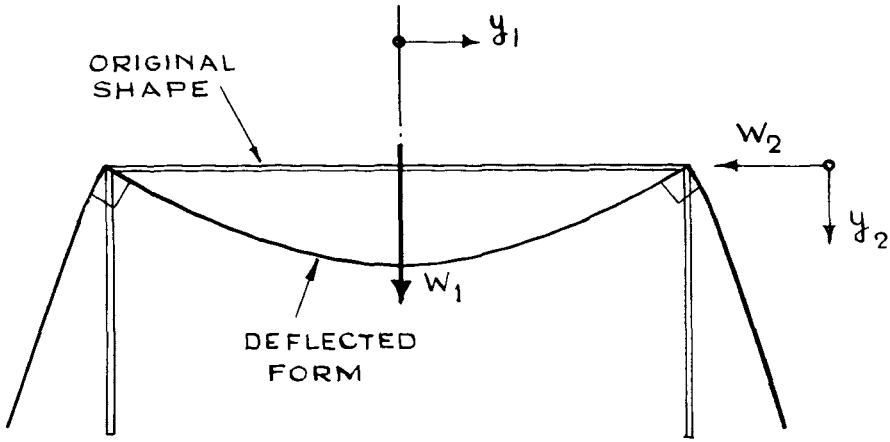

FIG. 2.

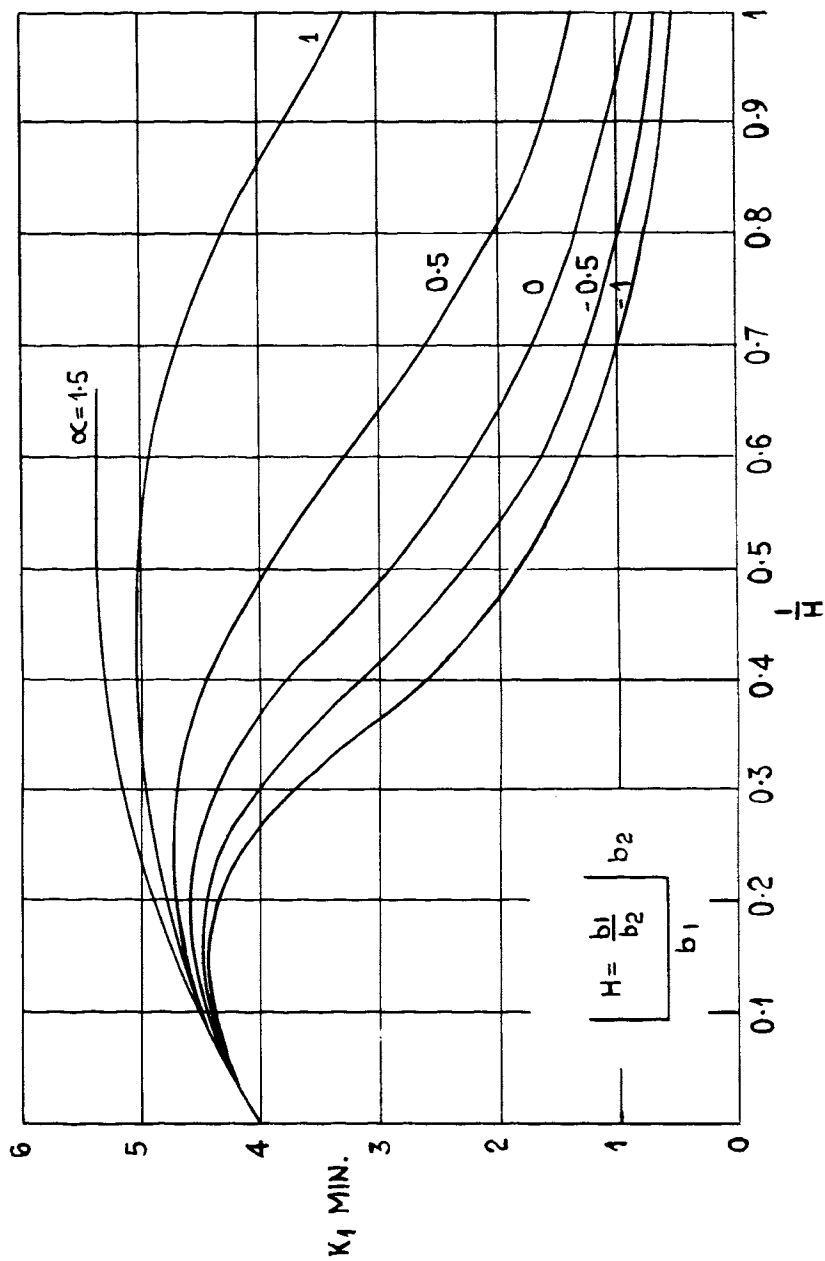
α=1·5
1
0·5
0
-0·5
-1
K1 MIN.
0
1
2
3
4
5
6
0·1
0·2
0·3
0·4
0·5
0·6
0·7
0·8
0·9
1
H
H= b1/b2
b1
b2

FIG. 3

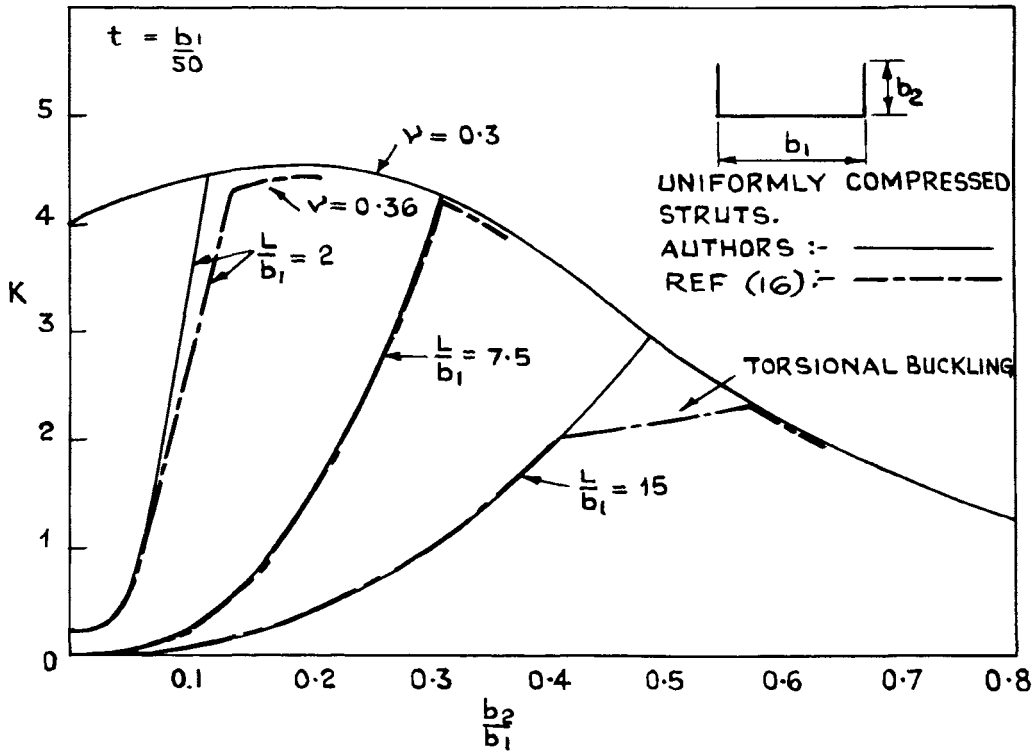
t = b1/50
ν = 0·3
ν = 0·36
L/b1 = 2
L/b1 = 7·5
L/b1 = 15
TORSIONAL BUCKLING
b2
b1
UNIFORMLY COMPRESSED STRUTS.
AUTHORS :-
REF (16) :-
K
0
1
2
3
4
5
0·1
0·2
0·3
0·4
0·5
0·6
0·7
0·8
b2/b1

FIG. 4

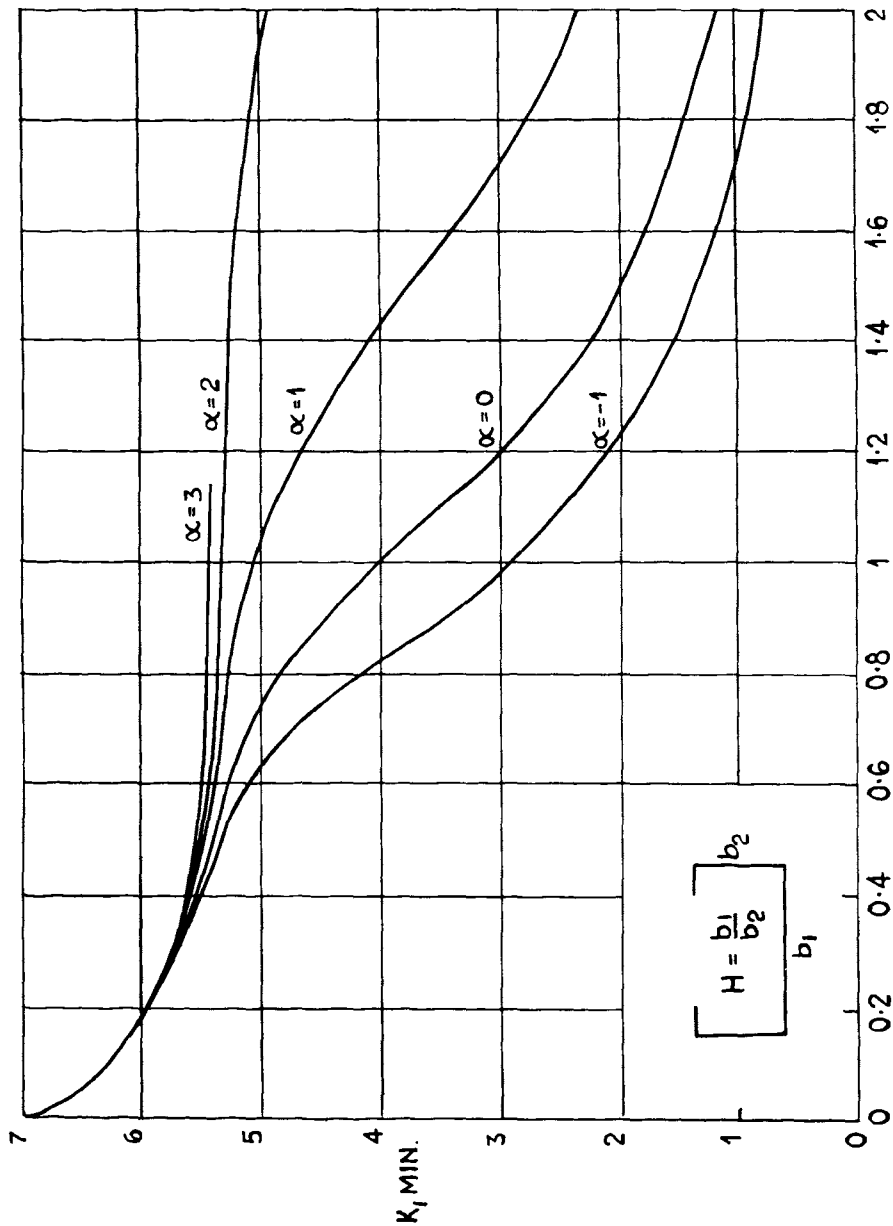
α=3
α=2
α=1
α=0
α=-1
K_1 MIN.
$\frac{1}{H}$
$H = \frac{b_1}{b_2}$
b_2
b_1
0
0·2
0·4
0·6
0·8
1
1·2
1·4
1·6
1·8
2
1
2
3
4
5
6
7

FIG 5.

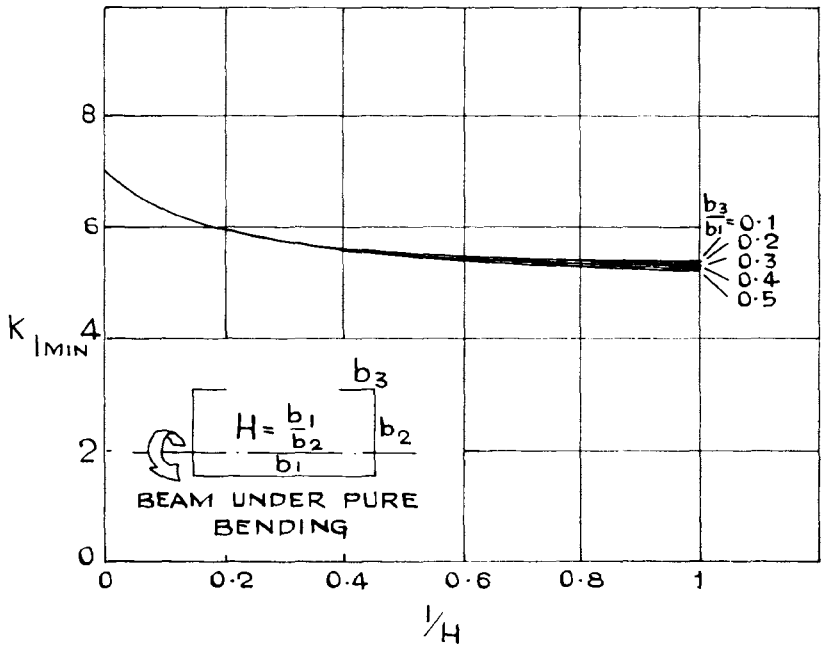
8
6
4
2
0
$K_{I_{MIN}}$
0
0·2
0·4
0·6
0·8
1
$1/H$
$\frac{b_3}{b_1}$ = 0·1
0·2
0·3
0·4
0·5
b_3
$H = \frac{b_1}{b_2}$
b_2
b_1
BEAM UNDER PURE BENDING

FIG. 6.

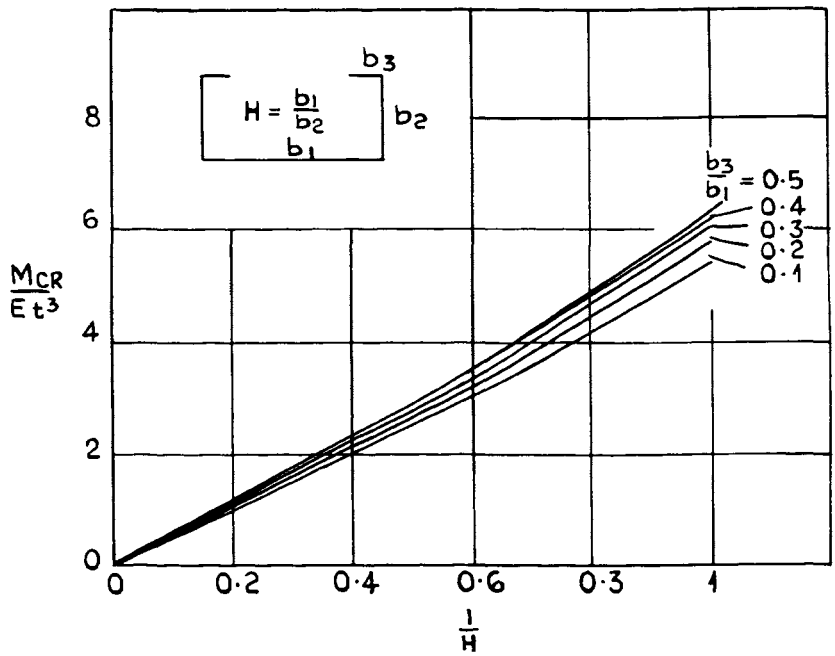

FIG 7

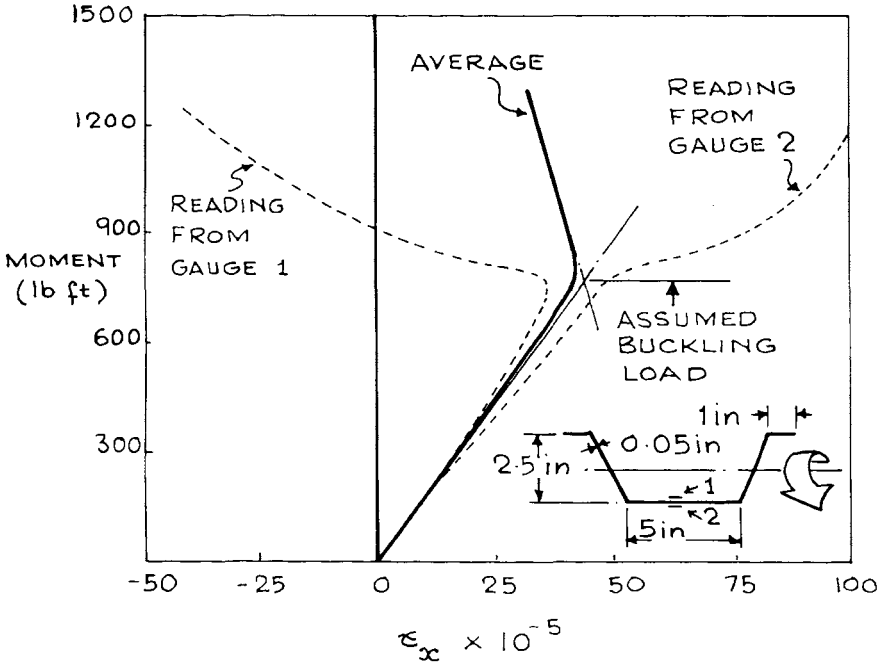
1500
1200
900
600
300
MOMENT
(lb ft)
AVERAGE
READING
FROM
GAUGE 2
READING
FROM
GAUGE 1
ASSUMED
BUCKLING
LOAD
1in
0·05in
2·5in
1
2
5in
-50
-25
0
25
50
75
100
$\varepsilon_x \times 10^{-5}$

FIG. 8.

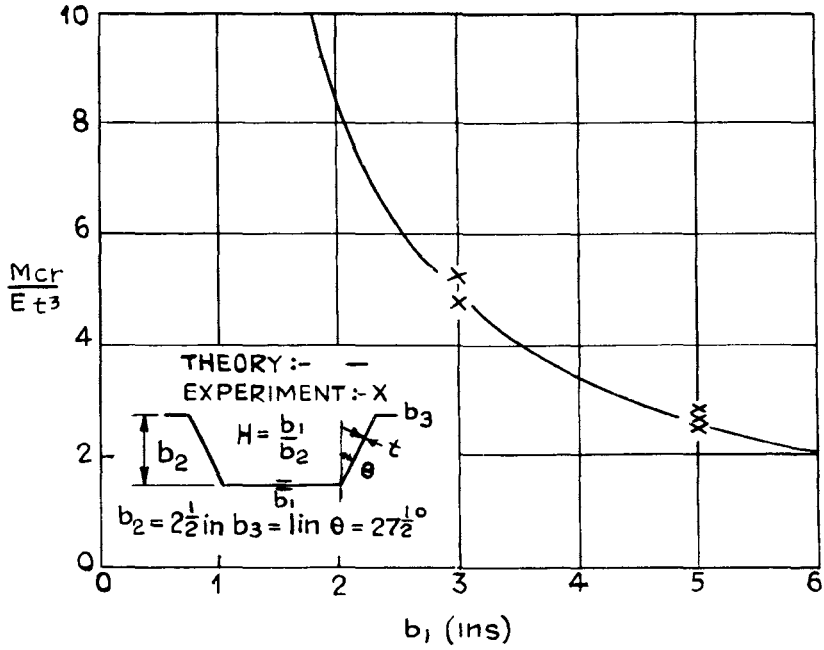
10
8
6
4
2
0
Mcr / E t³
THEORY :- —
EXPERIMENT :- X
b2
H = b1/b2
b3
t
θ
b1
b2 = 2½ in b3 = 1in θ = 27½°
0
1
2
3
4
5
6
b1 (ins)

FIG.9.

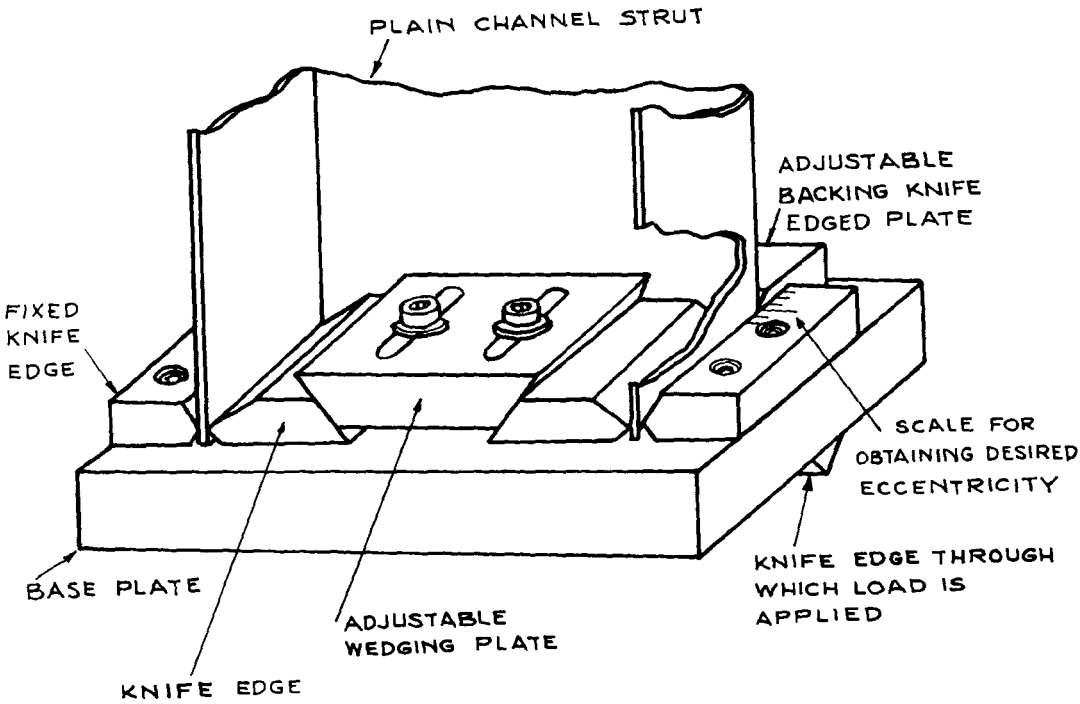

END PLATES FOR ECCENTRIC LOAD APPLICATION

FIG. 10

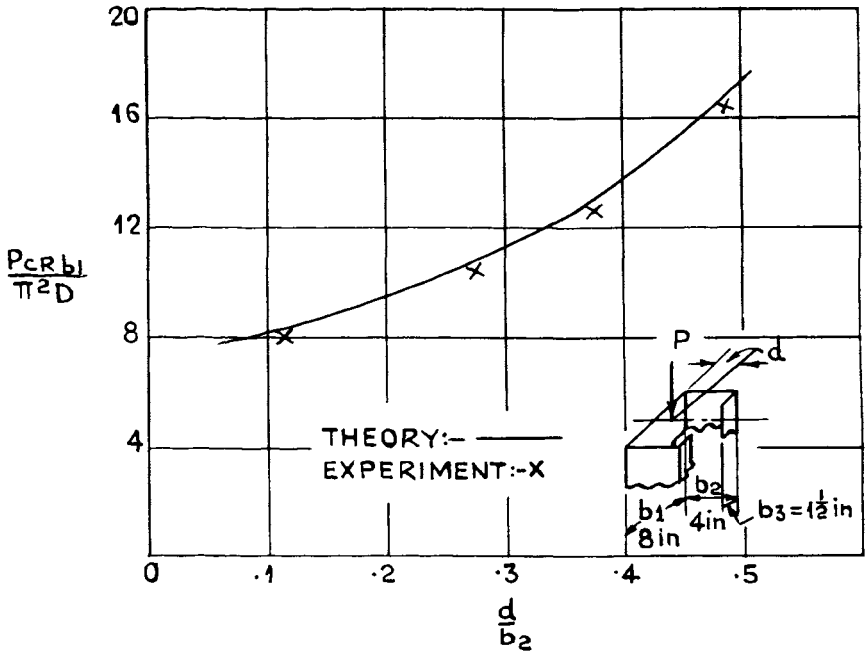
20
16
12
8
4
0
·1
·2
·3
·4
·5
$\frac{P_{CR}b_1}{\pi^2 D}$
$\frac{d}{b_2}$
THEORY:-
EXPERIMENT:-X
P
d
b_2
b_1
8in
4in
$b_3 = 1\frac{1}{2}$in

FIG 11

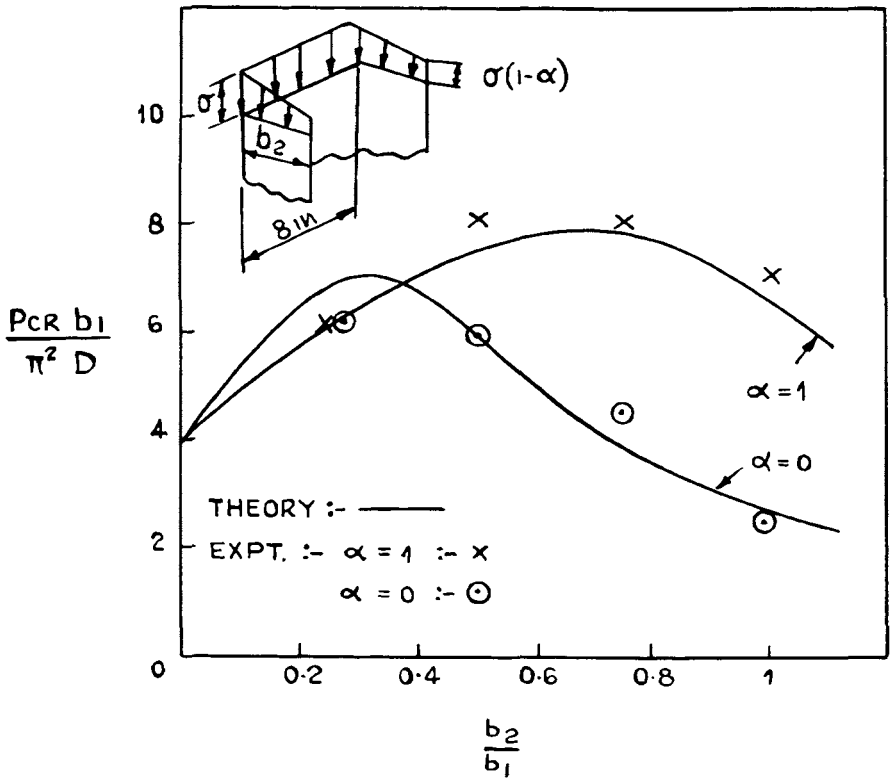
σ(1-α)
σ
b2
8in
10
8
6
4
2
0
PCR b1 / π² D
0·2
0·4
0·6
0·8
1
b2 / b1
α = 1
α = 0
THEORY :-
EXPT. :- α = 1 :- ×
α = 0 :- ⊙

FIG. 12.

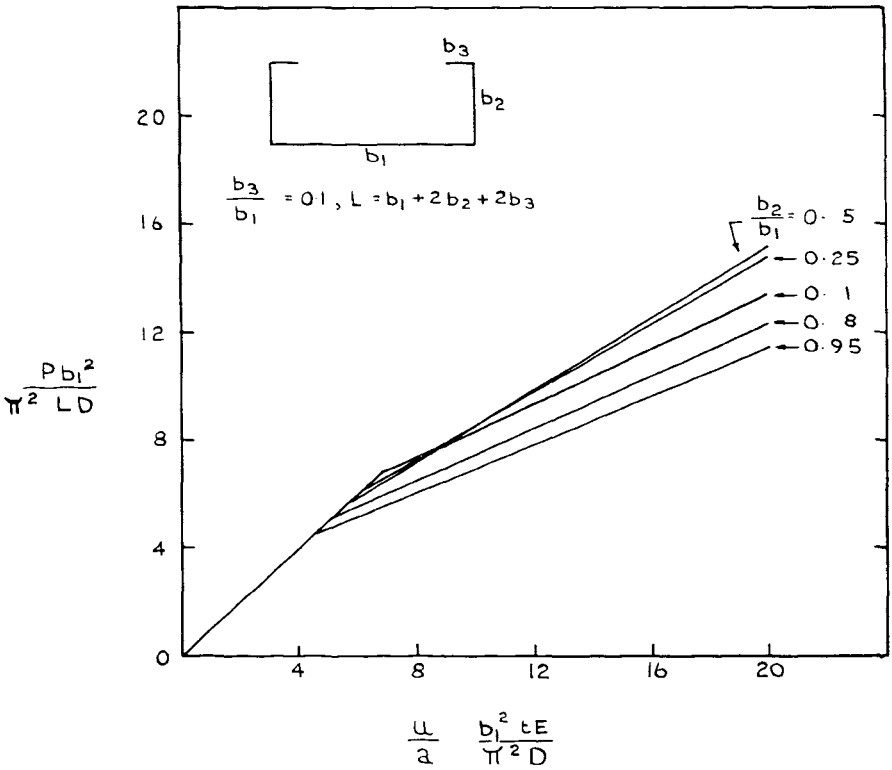
b3
b2
b1
b3/b1 = 0.1, L = b1 + 2b2 + 2b3
b2/b1 = 0.5
0.25
0.1
0.8
0.95
20
16
12
8
4
0
4
8
12
16
20
Pb1²/π² LD
u/a
b1² tE/π² D

FIG. 13

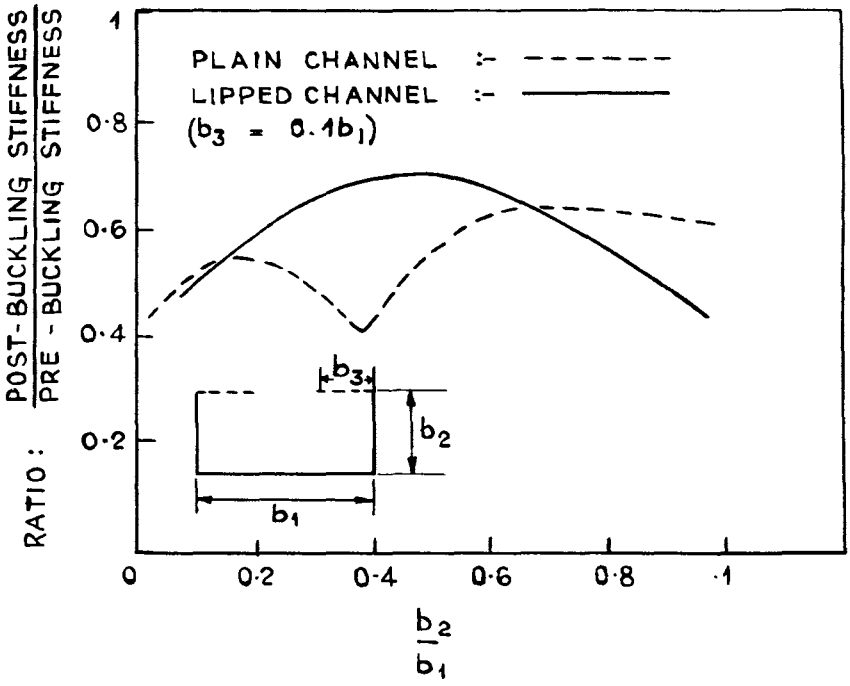
RATIO : POST-BUCKLING STIFFNESS / PRE-BUCKLING STIFFNESS
1
0·8
0·6
0·4
0·2
0
0·2
0·4
0·6
0·8
·1
PLAIN CHANNEL :-
LIPPED CHANNEL :-
(b3 = 0.1b1)
b3
b2
b1
b2/b1

FIG 14